Available online at www.sciencedirect.com
ScienceDirect
Carbohydrate Research 341 (2006) 2912–2920
Carbohydrate RESEARCH

Investigations into the role of oxacarbenium ions in glycosylation reactions by ab initio molecular dynamics

Andrei R. Ionescu,[a] Dennis M. Whitfield,[b,*] Marek Z. Zgierski[a] and Tomoo Nukada[c]

[a]*Steacie Institute for Molecular Sciences, NRC Canada, 100 Sussex Drive, Ottawa, Ont., Canada K1A 0R6*
[b]*Institute for Biological Sciences, NRC Canada, 100 Sussex Drive, Ottawa, Ont., Canada K1A 0R6*
[c]*Department of Fermentation Science, Faculty of Applied Bioscience, Tokyo University of Agriculture, Sakuragaoka, 1-1 Setagayaku, Tokyo 156-8502, Japan*

Received 10 May 2006; received in revised form 14 September 2006; accepted 21 September 2006
Available online 12 October 2006

Abstract—We present a constrained ab initio molecular dynamics method that allows the modeling of the conformational interconversions of glycopyranosyl oxacarbenium ions. The model was successfully tested by estimating the barriers to ring inversion for two 4-substituted tetrahydropyranosyl oxacarbenium ions. The model was further extended to predict the pathways that connect the $^4H_3$ half-chair conformation of 2,3,4,6-tetra-*O*-methyl-D-glucopyranosyl cation to its inverted $^5S_1$ conformation and the $^4H_3$ half-chair conformation of 2,3,4,6-tetra-*O*-methyl-D-mannopyranosyl cation to its inverted ^3E conformation. The modeled interconversion pathways reconcile a large body of experimental work on the acid-catalyzed hydrolysis of glycosides and the mechanisms of a number of glucosidases and mannosidases.

Keywords: Glycosylation; Oxacarbenium ions; Conformations

1. Introduction

The X-ray crystal structure of the glycosidase lysozyme led to the first proposal for an enzyme mechanism based on a protein structure.[1] This mechanism has as a central feature, a glycopyranosyl oxacarbenium ion intermediate with a $^4H_3$ half-chair conformation. Subsequent studies have proposed a second mechanism whereby a neutral enzyme-bound intermediate is separated from the reactants and products by two transition states (TS) with considerable oxacarbenium character.[2] This second mechanism must involve conformational changes of the glycopyranose ring to accommodate the planarity about the C-5–O-5–C-1–C-2 dihedral angle in the oxacarbenium ions. The oxacarbenium ion intermediates have very short lifetimes[3] and consequently their conformations have been primarily deduced from kinetic isotope effect (KIE) studies[4] or from biophysical studies of enzyme inhibitors combined with modeling.[5] The critical role of modeling for these studies naturally arises from the paucity of the experimental data. However, to date, no successful computational strategies to model the ring transformations of glycopyranoses, especially pseudorotation, have been developed. Typical approaches involve modeling snapshots along proposed pathways.[6] Such studies rely on a priori assumptions and hence can easily miss important features.

In the present work we show trajectories based on ab initio molecular dynamics (AIMD) studies of substituted glycopyranosyl oxacarbenium ions. AIMD trajectories naturally follow the free-energy surface,[7] and so the lowest energy ring conformational changes are found without a priori assumptions.[8] We have mapped our trajectories on to a sphere based on our description of the six-membered ring conformations.[9] We anticipate that our method can be applied to the modeling of any glycosyl-processing enzyme whose mechanism is thought to proceed through an oxacarbenium intermediate or TS. Such enzymes include most glycosidases[10]

* Corresponding author. Tel.: +1 613 993 5265; fax: +1 613 952 9092; e-mail: dennis.whitfield@nrc-cnrc.gc.ca

0008-6215/$ - see front matter © 2006 Elsevier Ltd. All rights reserved.
doi:10.1016/j.carres.2006.09.027

and most glycosyltransferases.[11] Our study is further anticipated to assist in the design and development of inhibitors for such enzymes.[12] The list of disease states and industrial processes to which such studies could be applied includes antivirals such as the neuramidase inhibitors like Tamiflu; bioethanol production from agricultural byproducts, and potential cancer drugs based on inhibitors of core 2 O-linked glycoprotein or 1,6-branched N-linked glycoprotein forming glycosyltransferases.[13]

Chemical glycosylation reactions are also thought to proceed through oxacarbenium ion intermediates.[14] Furthermore, it is thought that the conformational properties of these ions, at least in part, control the stereoselectivity of this important class of reactions.[15] One classic example that bears directly on the studies to be presented here was reported by Lemieux more than 50 years ago.[16] His research showed that the α/β isomeric 3,4,6-tri-*O*-acetyl-D-glucopyranosyl chlorides underwent solvolysis with a high degree of stereoselectivity. That is the α-chloride gave the β-acetate, and the β-chloride gave the α-acetate. Such stereoselectivity suggested an associative S_N2-like mechanism. Detailed kinetic studies for both isomers were entirely consistent with a S_N1-like mechanism. In order to rationalize this apparent anomaly, Lemieux invoked the possibility that the α-chloride ionized to a glucopyranosyl oxacarbenium with a $^4H_3$ ring conformation, and the β-chloride formed a similar ion, but with a $^3H_4$ ring conformation (Scheme 1). Further, he invoked that the two different ring conformations led to opposite facial selectivity leading to the observed products. To the best of our knowledge Lemieux was the first to propose multiple conformations of glycopyranosyl oxacarbenium ions. Some of these ideas have been recently revived to account for the stereoselectivity of C-glycosylation in which the assumption was made that the two oxacarbenium ion conformers rapidly interconvert and that stereoselectivity is determined by the facial selectivity of nucleophilic attack.[17]

Our group's previous study of the conformations of glycopyranosyl oxacarbenium ions by density functional theory (DFT) calculations including those for 2,3,4,6-tetra-*O*-methyl-D-glucopyranosyl (**1**) and 2,3,4,6-tetra-*O*-methyl-D-mannopyranosyl (**2**) oxacarbenium ions has consistently found at least two minima.[18] For (**1**), a $^4H_3$ half chair and a $^5S_1$ twist boat pair, whereas for (**2**), a $^4H_3$ half chair and a ^3E envelope pair were found (Scheme 2). If the ring conformations of these minima

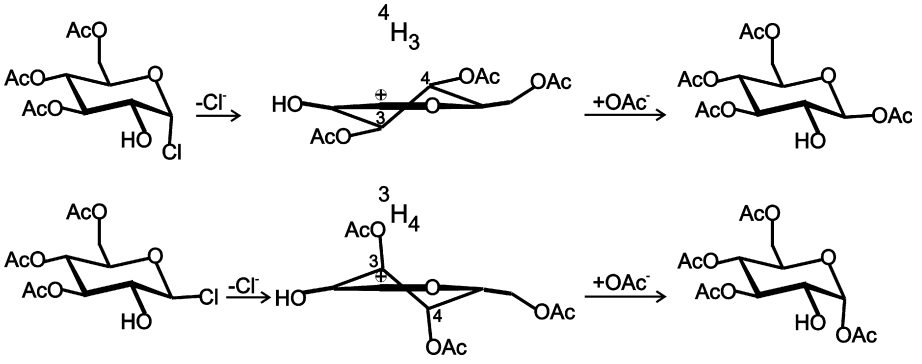

Scheme 1. Lemieux's two conformers of a D-glucopyranosyl oxacarbenium ion proposal to rationalize the experimental observation of the α-chloride (top) leading to the β-acetate and the β-chloride (bottom) leading to the α-acetate.

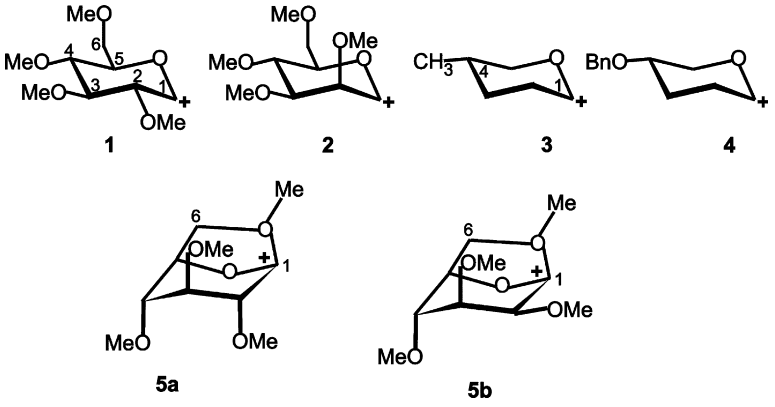

Scheme 2. Chemical structures and numbering of species **1** to **5**.

are represented on a sphere, as originally suggested by Hendrickson,[19] they are found on opposite hemispheres and on opposite (**2**) or nearly opposite faces (**1**) (see below). That is, interconversion in this representation, requires net movement about the equator (changing faces) and movement perpendicular to the equator (changing hemispheres). Our study seeks to find possible interconversion pathways between these minima. In particular we wish to assess if the barriers to interconversion are low enough to allow rapid equilibration.

We have developed a mathematical model that describes all pyranose conformations uniquely in terms of one chair, one boat, and one skew-boat conformation. Further, we have derived quantitative expressions for the characterization of the pyranose and other six-membered ring conformations. For details, see Supplementary data. The three internal coordinates (chair (q_1), boat (q_2), and skew boat (q_3)) defined in our previous papers can be applied as constraints in AIMD studies[20] of any six-membered ring inversion (q_1) or pseudorotation (q_2 and q_3).[21] Dynamical density functional theory (DFT) calculations were carried out with the projector augmented-wave (PAW) method of Blöchl, which is an implementation of the Car–Parrinello AIMD.[22] AIMD calculations were used to simulate the inversion/pseudorotation trajectories and to determine the free-energy difference along the reaction coordinate by thermodynamic integration of the average force on the constraint at a given temperature. The reported static calculations were carried out with the GAUSSIAN 98 program package. The static calculations were employed as a complement for the dynamical simulations and to derive the enthalpies of reaction, which are sometimes available from experimental data. Further computational details are presented in Supplementary data available in the electronic version of this paper.

2. Results

Before engaging in a detailed study of **1** and **2**, we wanted to validate our methodology by studying an example with a firm experimental basis.

A recent publication by the Woerpel group convincingly demonstrated that both the 4-methyltetrahydropyranosyl (**3**) and 4-benzyloxytetrahydropyranosyl (**4**) oxacarbenium ions can undergo ring inversion under their reaction conditions before nucleophilic attack.[23] Furthermore, both **3** and **4** exhibit facial selectivity based on a preferred 4-methyl pseudoequatorial conformation for **3** and a preferred 4-benzyloxy pseudoaxial conformation for **4**.[24] Based on least motion arguments, both ions are expected to be formed in a $^3H_4$ half-chair conformation, which can then interconvert. That is, the chosen chemical reaction conditions allow for ionization to the oxacarbenium ion, followed by ring inversion and subsequent facially selective nucleophilic attack.

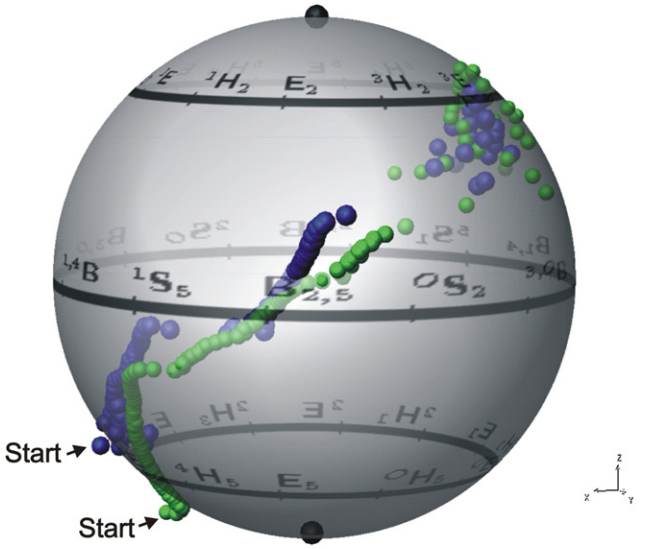

Figure 1. AIMD trajectories for 4-methyltetrahydropyranosyl (green) and 4-hydroxytetrahydropyranosyl (blue) oxacarbenium ions mapped onto the conformational sphere.

Our slow growth in vacuo AIMD trajectories (see the 'Free energy' section in supplementary data) using the chair constraint q_1 to drive the conformational change are plotted in Figure 1 (green for **3** and blue for the hydroxyl analogue of **4**). The trajectories clearly show that both derivatives invert along a similar pathway. Starting from the $^4H_3$ half chair, both trajectories proceed along the surface of the sphere toward the $^3H_4$ half-chair conformation (^4E for **3**). Both trajectories consist of a mixture of inversion and pseudorotation. In order to eliminate the inherent errors arising from the slow growth approximation, about 150 selected points were reoptimized with their ring dihedral angles frozen as shown in Figure 2.

The conformational energy differences (Fig. 3) obtained by full optimization clearly support Woerpel's experimental results and show a pseudoequatorial preference for **3** and a pseudoaxial preference for **4**. In further agreement with the experiment are the calculated inversion barriers of about 17 kJ mol^{-1} from the $^3H_4$ or ^4E minima, which are low enough to allow rapid equilibration under the experimental conditions. The 35 kJ mol^{-1} to get out of the pseudoaxial $^4H_3$ minimum for **4** also corroborates the preferred nucleophilic attack on this species. All the important energies are compiled for the reaction starting from $^3H_4$ or ^4E in Table 1 and from $^4H_3$ in Table 2 as determined from the different calculations in order to allow an assessment of their accuracy. The TS for interconversion is predicted to be near an $^OS_2$ skew-boat conformation. Note that this differs considerably from cyclohexane inversion and pseudorotation, which have TSs with half-chair or boat conformations, respectively. The current experimental evidence does not allow determination of the conforma-

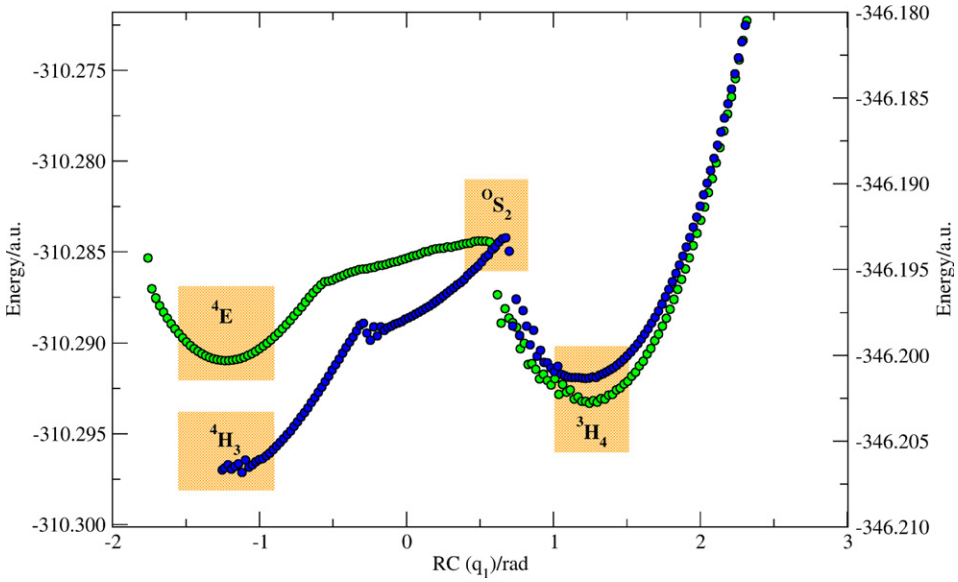

Figure 2. Static DFT (B3LYP and 6-311+G**) potential energy surfaces for the transition $^4H_3$ to $^3H_4$ of 4-methyltetrahydropyranosyl (green) and 4-hydroxytetrahydropyranosyl (blue). 1 a.u. = 2625.4985 kJ mol^{-1}.

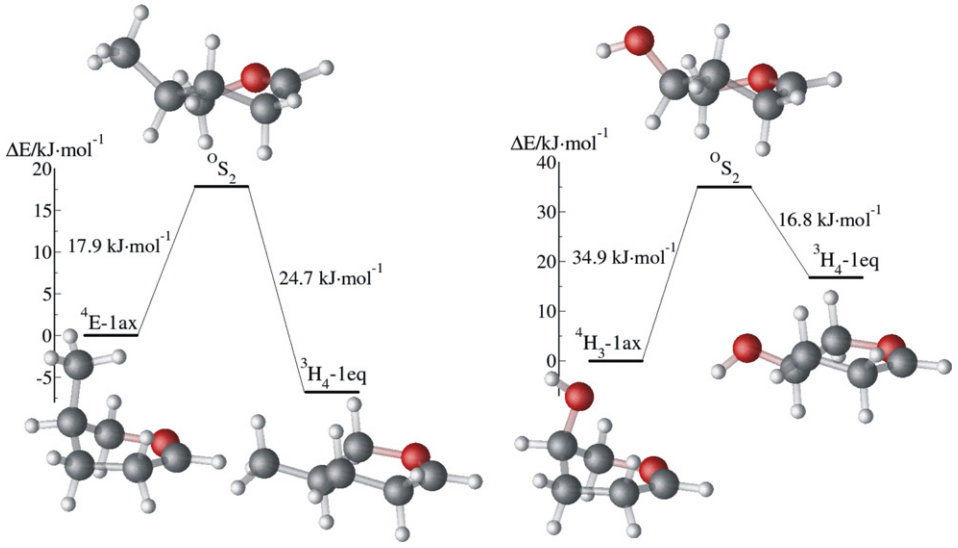

Figure 3. Energetics for 4-methyltetrahydropyranosyl (left) and 4-hydroxytetrahydropyranosyl (right) inversion.

Table 1. Energy barriers for 4-methyltetrahydropyranosyl and 4-hydroxytetrahydropyranosyl $^4E/^4H_3$ to $^3H_4$ inversion in kJ mol^{-1}at 0 K

Compound	ΔG PAW	ΔG Opt	ΔH Opt	ΔE Opt	ΔE Static frozen dihedrals
4-Methyl-THP	14.5	19.0	15.2	17.1	18.4
4-Hydroxy-THP	28.4	31.3	28.7	30.1	34.1

Table 2. Energy barriers for 4-methyltetrahydropyranosyl and 4-hydroxytetrahydropyranosyl $^3H_4$ to $^4E/^4H_3$ inversion in kJ mol^{-1} at 0 K

Compound	ΔG PAW	ΔG Opt	ΔH Opt	ΔE Opt	ΔE Static frozen dihedrals
4-Methyl-THP	9.8	25.9	21.6	23.7	23.6
4-Hydroxy-THP	6.1	19.9	13.7	16.1	21.0

tion of this proposed TS. All the stationary points for **3** and **4** were validated by calculation of the Hessian. Furthermore, a normal mode analysis of the imaginary frequency associated with the TS conformations shows that the leading components were ring deformations. A detailed analysis of this mode is presented in Supplementary data accompanying this paper. Thus if ions like **1** or **2** conformationally equilibrate under glycosylation conditions, the barriers to equilibration should be about 17 kJ mol^{-1}or less.

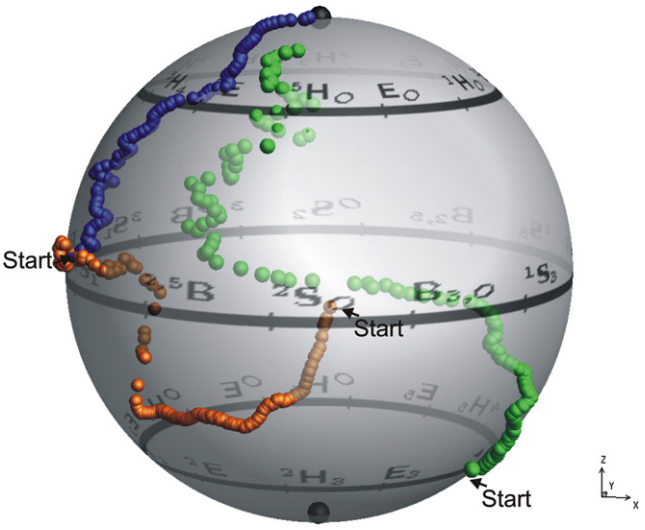

Figure 4. AIMD trajectories for 2,3,4,6-tetra-*O*-methyl-D-glucopyranosyl oxacarbenium ions mapped onto the conformational sphere: green $^{4}H_{3}$ (q_1), blue $^{2}S_{O}$ (q_1), and orange $^{2}S_{O}$ (q_2).

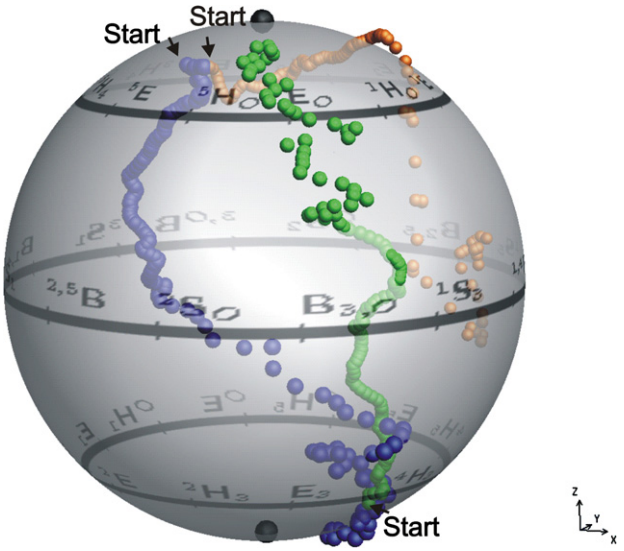

Figure 6. AIMD trajectories for 2,3,4,6-tetra-*O*-methyl-D-mannopyranosyl oxacarbenium ion mapped onto the conformational sphere: green $^{4}H_{3}$ (q_1), blue ^{3}E (q_1), and orange ^{3}E (q_2).

A similar AIMD study for **1** is presented in Figures 4, 5, and 8, and for **2** in Figures 6–8. In total 12 AIMD simulations using q_1, q_2 and q_3 were performed to fully explore the PES for **1** and **2**. We present the six simulations that connect the two minima for each compound that was previously found. The six studies not shown found no additional minima or TSs. The important energy barriers are compiled in Table 3.

First, a q_1 constrained trajectory starting from $^{4}H_{3}$ for **1** (green in Fig. 4) stays close to the surface of the sphere and does not appreciably pseudorotate until it approaches the equator with a change from near $^{1}S_{3}$ rotating to near $^{2,5}B$ before moving up toward $^{1}C_{4}$. Note that the representation onto the conformational sphere stops near the $^{5}H_{O}$ conformation, beyond this point the trajectory leaves the surface of the sphere before reaching the $^{1}C_{4}$ conformation. This out of the sphere's surface part of the trajectory is due to the formation of a 1,6-anhydro O–C bond (**5a**) (see below). Second, a q_2 trajectory (orange in Fig. 4) starting from $^{2}S_{O}$ exhibits the not predictable behavior of moving toward $^{4}C_{1}$ and not along

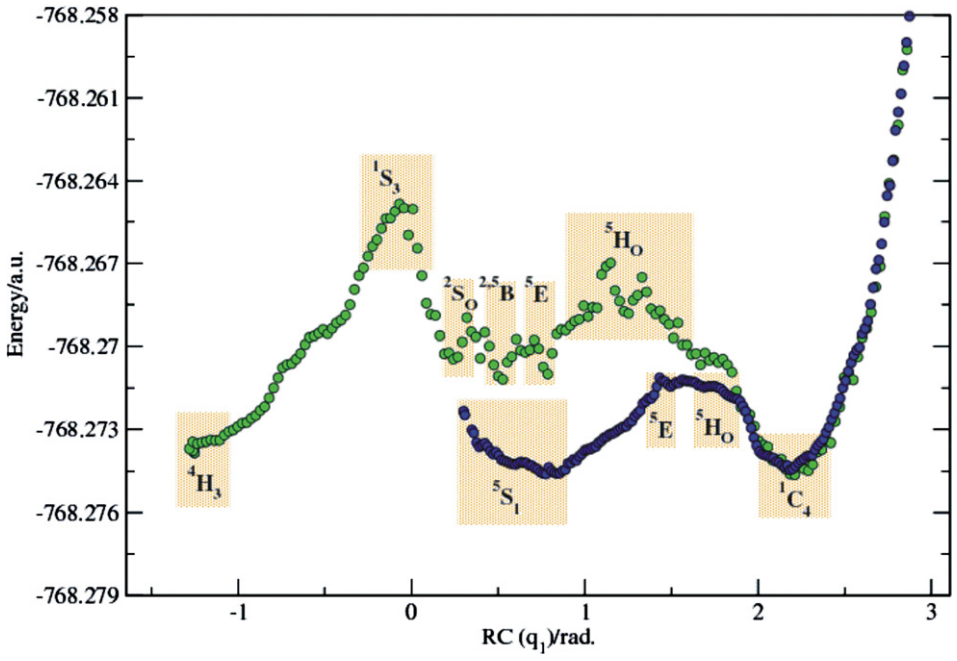

Figure 5. Static DFT (B3LYP and 6-311+G**) potential energy surfaces for the transition $^{4}H_{3}$ to $^{1}C_{4}$ (green) and $^{5}S_{1}$ to $^{1}C_{4}$ (blue) of 2,3,4,6-tetra-*O*-methyl-D-glucopyranosyl oxacarbenium ion. 1 a.u. = 2625.4985 kJ mol^{-1}.

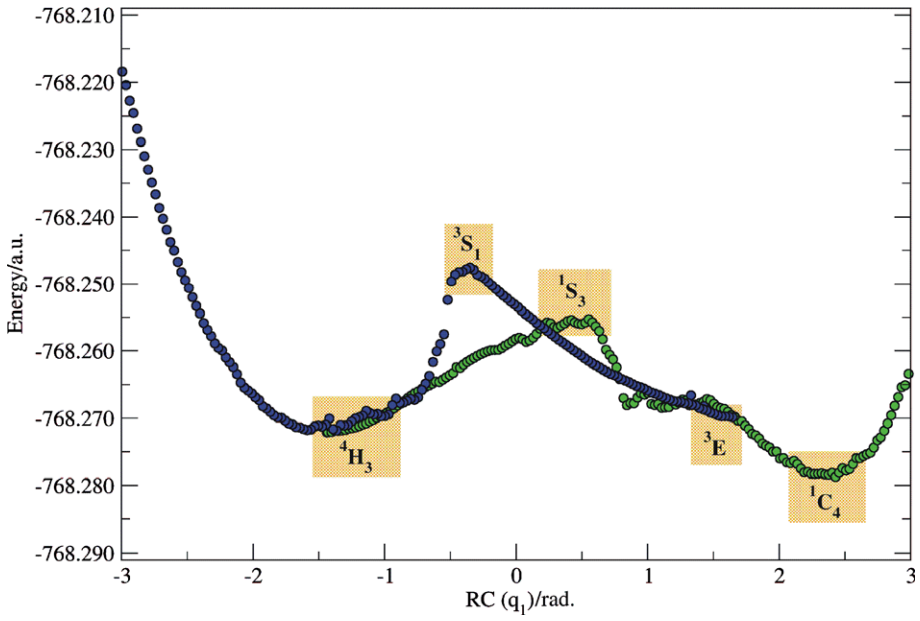

Figure 7. Static DFT (B3LYP and 6-311+G**) potential energy surfaces for the transition $^4H_3$ to $^1C_4$ (green) and ^3E to $^4H_3$ (blue) of 2,3,4,6-tetra-*O*-methyl-D-mannopyranosyl oxacarbenium ion. 1 a.u. = 2625.4985 kJ mol^{-1}.

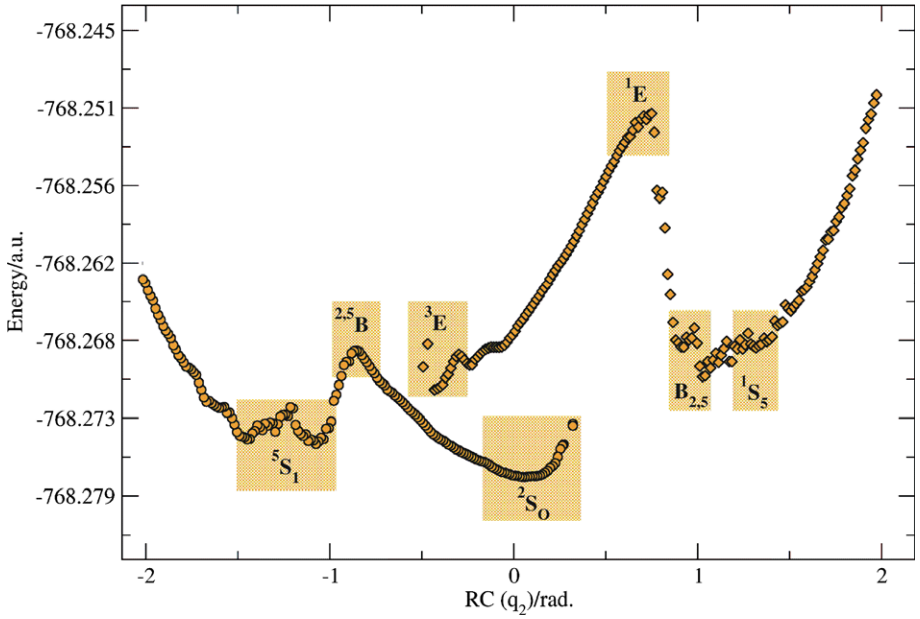

Figure 8. Static DFT (B3LYP and 6-311+G**) potential energy surfaces for the pseudorotation ^2S_O to $^5S_1$ (circles) and ^3E to $^1S_5$ (diamonds) of 2,3,4,6-tetra-*O*-methyl-D-glucopyranosyl and 2,3,4,6-tetra-*O*-methyl-D-mannopyranosyl oxacarbenium ions, respectively. 1 a.u. = 2625.4985 kJ mol^{-1}.

the equator before pseudorotating and then moving back to the equator to $^{2,5}B$ and then to the second global minimum at $^5S_1$. Third, a trajectory (blue in Fig. 4) starting from $^5S_1$ moves straight toward $^1C_4$. No minimum is found near $^3H_4$, further confirming the previous static calculations, which did not find stable conformations in this region of the conformational space.

The energetics of the q_1 and q_2 trajectories for **1** are shown in Figures 5 and 8, respectively. Analysis of the energetic curves points out some interesting properties. First, there is a third minimum near $^1C_4$, which is the result of 1,6-anhydro bond formation (**5a**). Products derived from such species are frequently isolated by synthetic chemists,[25] and at least one class of glycosidases, the bacterial soluble lytic transglycosidases produce 1,6-anhydro-D-*gluco*-configured sugars as products.[26] The change from oxacarbenium ion to dioxacarbenium ion is the source of the stabilization, which overwhelms

Table 3. Energy barriers for 2,3,4,6-tetra-*O*-methyl-D-glycopyranosyl inversions in kJ mol^{-1} at 0 K

Inversion	ΔE Static frozen dihedrals (2,3,4,6-tetra-*O*-methyl D-glucopyranosyl)	ΔE Static frozen dihedrals (2,3,4,6-tetra-*O*-methyl-D-mannopyranosyl)
$^4H_3$ to $^1C_4$	23.6	44.6
	21.0[a]	60.4[a]
$^5S_1$ to $^1C_4$	10.5	—
	10.5[a]	—
^3E to $^4H_3$	—	57.7
	—	63.0[a]
^2S_O to $^5S_1$	23.6	—
	18.4[a]	—
^3E to $^1S_5$	—	52.5
	—	49.9[a]

[a] Energy barrier for the reverse inversion.

the unfavorable ring conformation. Second, the energy barrier from the minima on the pseudorotational itinerary (Fig. 5, green curve) to the 1,6-anhydro-D-*gluco*-configured $^1C_4$ conformation is less than half of the energy barrier from the $^4H_3$ minimum to the conformations situated on the equator. Third, the energy barrier for the pseudorotation (23.6 kJ mol^{-1}) has a comparable value with the energy barrier for the inversion (23.6 kJ mol^{-1}).

Two q_1 trajectories are shown for **2**, one starting from $^4H_3$ (green in Fig. 6) and one starting from ^3E (blue in Fig. 6). Both cross the equator of the sphere and have maxima near $^1S_3$ (green in Fig. 7) and $^3S_1$ (blue in Fig. 7). A q_2 trajectory starting from ^3E (orange in Fig. 6) starts with pseudorotation as might be expected, but near ^1E it moves on the inside of the sphere toward the equator, ending near the $^1S_5$ conformation.

The energetics of the q_1 and q_2 trajectories for **2** are shown in Figures 7 and 8, respectively, and also show three properties. First, as for **1** there is a third minimum (Fig. 7) in addition to $^4H_3$ and ^3E minima near the $^1C_4$ conformation leading to 1,6-anhydro-dioxolenium ion formation (**5b**). Second, similarly to the energetics in **1**, the energy barrier for the formation of the dioxolenium ion is lower than the energy barrier for the inversion. Third, the pseudorotation curve for **2** (Fig. 8) has a much steeper slope than for **1**.

In all the above results the value of the energy barriers for *gluco*-configured oxacarbenium ions was approximately half the corresponding value of the *manno*-configured oxacarbenium ions, see Table 3. The values for **1** are low enough that rapid equilibration is expected whereas for **2** facile equilibration is less likely.

3. Discussion

Hydrolysis of glycosides, whether chemically catalyzed by acid or by acid catalysis induced by glycosidases, as discussed above, are thought to proceed through glycopyranosyl oxacarbenium ion TSs. Similarly, many variants of the reverse glycosylation reaction are thought to proceed through oxacarbenium ion intermediates or TSs. In the case of six-membered rings in particular, there are two mechanistic extremes for how the conformation of the ion can be formed. In one mechanism the neutral species changes to a reactive conformation, followed by loss of a leaving group leading to the oxacarbenium ion. Protonation or Lewis acid complexation of the departed leaving group prevents the back reaction. Least motion arguments suggest that α-glucosides following this mechanism should ionize to a $^4H_3$ conformation, whereas based on coplanar stereoelectronic arguments β-glycosides should first pass through a boat conformation such as $B_{3,O}$ or $^{1,4}B$ before ionization. Once ionized, and if the species have sufficient lifetime, then they may interconvert following pathways like those we have calculated. In the second mechanistic extreme, ionization occurs in a conformation at or near the starting stable conformation, which is usually a chair conformation for glycopyranosyl compounds, followed by ring change to the most stable oxacarbenium ion conformation, that is, one of the minima described above for ions configured similar to **1** or **2**. In this case protonation or Lewis acid complexation induces loss of the leaving group.

In a previous publication we have mapped the inversion pathway for the neutral α/β isomeric 1,2,3,4,6-penta-*O*-methyl-D-glucopyranosides.[21] For both α and β glucopyranosides the pathways we found pass through similar but not identical ^OE TSs to $^OS_2$ twist boat secondary minima. Since these conformations are far from the conformations we find for **1**, it appears that some bond breaking likely accompanies ring conformational changes leading to oxacarbenium ion formation. That is, the second mechanistic extreme is most consistent with our calculations. A previous AIMD study using a C-1-nucleophile bond length as constraint also supports a mechanism where protonation of the leaving group triggers a coupled series of events leading to oxacarbenium ion formation, that is, closest to the second mechanistic extreme.[27]

Only a small amount of direct experimental evidence is available about the conformations of glycopyranosyl oxacarbenium ions. One notable example is an analysis that combines KIE measurements of the acid-catalyzed hydrolysis of the α/β methyl glycosides of D-glucopyranose accompanied by forcefield-based modeling, which was interpreted to indicate a 'flattened toward planarity $^1S_3$ skew boat' TS for α-hydrolysis and a 'flattened $^{2,5}B$ boat' TS for β-hydrolysis.[28] Since our calculations have minimal intrinsic bias, it is significant that both of these conformations are found on our trajectories at or near stationary points, that is, $^1S_3$ on a q_1 trajectory and $^{2,5}B$ on a q_2 trajectory. These results are consistent with a pathway that proceeds through a $^4H_3$ conformation

for α-hydrolysis and a $B_{3,O}$ or similar conformation, which pseudorotates to $^{2,5}B$ for β-hydrolysis.

We also thought it was of considerable interest to see if postulated TSs for glycosyl-processing enzymes could be found on our AIMD trajectories, as this would suggest that Nature at least in some cases makes use of these low-energy pathways. For example, *Clostridium thermocellum* contains an inverting β-glucosidase, which has been suggested to have a $^{2,5}B$ TS consistent with the acid-catalyzed pathway described above.[29] On the other hand, the retaining β-glucosidase from *Bacillus agaadhaerens* is proposed to use a $^{1}S_3$ TS, suggesting a mechanism with an early ionization to a $^{4}H_3$ conformation, followed by a $^{1}S_3$ TS.[30] The *Thermobifida fusca* glucosidase is reported to have a $^{2}S_O$ TS, which is in between the $B_{3,O}$ and $^{2,5}B$ on our q_2 trajectory.[31] The retaining β-D-gluco- (and D-galacto-)sidases from *Sulfolobus solfataricus* has been proposed to have a $^{4}H_3$ TS,[32] and the barley β-D-glucosidase an ^{4}E near $^{4}H_3$ TS.[33] These two enzymes therefore appear to have TSs earlier in the pathway. All of these postulated TSs can be found on the green curve in Figure 5. Since there is no a priori reason to expect this correlation between our AIMD trajectories and the conformations of TSs, we interpret this correlation as evidence for the soundness of our computational approach.

The class I and class II α-mannosidases involved in N-linked glycoprotein quality control likely use conformational pathways that differ considerably.[34] For class 1 enzymes, a $^{1}S_3$ TS has been proposed, which is on our q_1 trajectory that starts from ^{3}E. In this case, a preionization ring conformational change is likely.[35] On the contrary, class 2 enzymes have been proposed to have a TS between $^{1,4}B$ and $^{4}H_3$. These observations strongly suggest that inhibitors selective for each class of enzymes can be found.[36] Finally a β-mannanase has been reported to have a $B_{2,5}$ TS, which is clearly seen to be a minimum in the q_2 trajectory of **2**.[37] The adjacent $^{1}S_5$ conformation is linked by a facile pseudorotation and could also be considered. A similar difference in pathways[38] has been reported for class 10 and class 11 xylanases.[39] Again, it seems probable that these conformational differences could be used to develop selective inhibitors.[40]

The trajectories presented here are consistent with a variety of experimental observations, and useful insights into how to design glycosidase inhibitors can be gleaned from this data. It is anticipated that if these AIMD trajectories are incorporated into a quantum mechanical/molecular mechanics framework where the residues of the active site and the exact substrate of the enyzme are modeled, then even more detailed conformational data can be found that can be used for inhibitor design. In this way the first attempts by Phillips to deduce mechanism from protein structure based on a series of snapshots can now be extended to examining the dynamical pathways.

4. Conclusions

The goal of this paper was to investigate the conformational interconversions of glycopyranosyl oxacarbenium ions in both dynamical and static calculations. We have combined the constrained method with ab initio molecular dynamics simulations to fully sample the potential energy surface of two 4-substituted tetrahydropyranosyl oxacarbenium ions and 2,3,4,6-tetra-*O*-methyl-D-gluco- and mannopyranosyl cations. The inversion process was conducted via q_1, q_2, and q_3 constraints. The AIMD inversion pathways evidenced minima situated on smaller radius circles, halfway between the pseudorotational itinerary (the equator of the conformational sphere) and the two chair conformations (the poles of the conformational sphere), and transition states situated on the pseudorotational itinerary. Recent thinking on the topic of enzymatic TSs emphasizes the need to develop dynamic descriptions of TSs.[41] We consider our results a major step toward achieving this goal for carbohydrate-processing enzymes, as our method naturally allows for pseudorotation, which must occur at or near the TS of many of these enzymes.

Acknowledgment

This work was supported by the High-Performance Computing initiative of the NRC Canada. This is NRC paper #42511.

Supplementary data

Supplementary data associated with this article can be found, in the online version, at doi:10.1016/j.carres.2006.09.027.

References

1. Phillips, D. C. *Proc. Natl. Acad. Sci. U.S.A.* **1967**, *57*, 484–495.
2. Vocadlo, D. J.; Davies, G. J.; Laine, R.; Withers, S. G. *Nature* **2001**, *412*, 835–838.
3. Banait, N. S.; Jencks, W. P. *J. Am. Chem. Soc.* **1991**, *113*, 7951–7958.
4. Crich, D.; Chandrasekera, N. S. *Angew. Chem., Int. Ed.* **2004**, *43*, 5886–5889.
5. Davies, G. J.; Ducros, V. M. A.; Varrot, A.; Zechel, D. L. *Biochem. Soc. Trans.* **2003**, *31*, 523–527.
6. Kankainen, M.; Laitinen, T.; Peräkylä, M. *Phys. Chem. Chem. Phys.* **2004**, *6*, 5074–5080.
7. Car, R.; Parrinello, M. *Phys. Rev. Lett.* **1985**, *55*, 2471–2474.
8. Yang, S.; Hristov, I.; Fleurat-Lessard, P.; Ziegler, T. *J. Phys. Chem. A* **2005**, *109*, 197–204.
9. Bérces, A.; Nukada, T.; Whitfield, D. M. *Tetrahedron* **2001**, *57*, 477–491.
10. Ganem, B.; Papandreou, G. *J. Am. Chem. Soc.* **1991**, *113*, 8984–8985.

11. Ünligil, U. M.; Rini, J. M. *Curr. Opin. Struct. Biol.* **2000**, *10*, 510–517.
12. Zhou, G. C.; Parikh, S. L.; Tyler, P. C.; Evans, G. B.; Furneaux, R. H.; Zubkova, O. V.; Benjes, P. A.; Schramm, V. L. *J. Am. Chem. Soc.* **2004**, *126*, 5690–5698.
13. *Carbohydrate-based Drug Discovery*; Wong, C. H., Ed.; Wiley-VCH: Weinheim, 2003.
14. Boebel, T. A.; Gin, D. Y. *J. Org. Chem.* **2005**, *70*, 5818–5826.
15. Nukada, T.; Bérces, A.; Whitfield, D. M. *Carbohydr. Res.* **2002**, *337*, 765–774.
16. Lemieux, R. U.; Huber, G. *Can. J. Chem.* **1954**, *33*, 128–133.
17. Lucero, C. G.; Woerpel, K. A. *J. Org. Chem.* **2006**, *71*, 2641–2647.
18. Nukada, T.; Bérces, A.; Wang, L. J.; Zgierski, M. Z.; Whitfield, D. M. *Carbohydr. Res.* **2005**, *340*, 841–852.
19. Hendrickson, J. B. *J. Am. Chem. Soc.* **1967**, *26*, 7047–7061.
20. Bérces, A.; Enright, A. G.; Nukada, T.; Whitfield, D. M. *J. Am. Chem. Soc.* **2001**, *123*, 5460–5464.
21. Ionescu, A. R.; Bérces, A.; Zgierski, M. Z.; Whitfield, D. M.; Nukada, T. *J. Phys. Chem. A* **2005**, *109*, 8096–8105.
22. Blöchl, P. E. *Phys. Rev. B* **1994**, *50*, 17953–17979.
23. Shenoy, S. R.; Woerpel, K. A. *Org. Lett.* **2005**, *7*, 1157–1160.
24. Chamberland, S.; Ziller, J. W.; Woerpel, K. A. *J. Am. Chem. Soc.* **2005**, *127*, 5322–5323.
25. *Levoglucosenone and Levoglucosans: Chemistry and Applications*; Witczak, Z. J., Ed.; ATL Press, Inc. Science Publishers: Mount Prospect, Il, 1994.
26. Van Asselt, E. J.; Thunnissen, A. M. W. H.; Dijkstra, B. W. *J. Mol. Biol.* **1999**, *291*, 877–898.
27. Stubbs, J. M.; Marx, D. *Chem. Eur. J.* **2005**, *11*, 2651–2659.
28. Bennet, A. J.; Sinnott, M. L. *J. Am. Chem. Soc.* **1986**, *108*, 7287–7294.
29. Guérin, D. M. A.; Lascombe, M. B.; Costabel, M.; Souchon, H.; Lamzin, V.; Béguin, P.; Alzari, P. M. *J. Mol. Biol.* **2002**, *316*, 1061–1069.
30. Davies, G. J.; Mackenzie, L.; Varrot, A.; Dauter, M.; Brzozowski, A. M.; Schülein, M.; Withers, S. G. *Biochemistry* **1998**, *37*, 11707–11713.
31. Larsson, A. M.; Bergfors, T.; Dultz, E.; Irwin, D. C.; Roos, A.; Driguez, H.; Wilson, D. B.; Jones, T. A. *Biochemistry* **2005**, *44*, 12915–12922.
32. Gloster, T. M.; Roberts, S.; Ducros, V. M. A.; Perugino, G.; Rossi, M.; Hoos, R.; Moracci, M.; Vasella, A.; Davies, G. J. *Biochemistry* **2004**, *43*, 6101–6109.
33. Hrmova, M.; Streltsov, V. A.; Smith, B. J.; Vasella, A.; Varghese, J. N.; Fincher, G. B. *Biochemistry* **2005**, *44*, 16529–16539.
34. Karaveg, K.; Siriwardena, A.; Tempel, W.; Liu, Z. J.; Glushka, J.; Wang, B. C.; Moremen, K. W. *J. Biol. Chem.* **2005**, *280*, 16197–16207.
35. Karaveg, K.; Moremen, K. W. *J. Biol. Chem.* **2005**, *280*, 29837–29848.
36. Shah, N.; Kuntz, D. A.; Rose, D. R. *Biochemistry* **2003**, *42*, 13812–13816.
37. Ducros, V. M. A.; Zechel, D. L.; Murshudov, G. N.; Gilbert, H. J.; Szabó, L.; Stoll, D.; Withers, S. G.; Davies, G. J. *Angew. Chem., Int. Ed.* **2002**, *41*, 2824–2827.
38. Williams, S. J.; Hoos, R.; Withers, S. G. *J. Am. Chem. Soc.* **2000**, *122*, 2223–2235.
39. Sidhu, G.; Withers, S. G.; Nguyen, N. T.; McIntosh, L. P.; Ziser, L.; Brayer, G. D. *Biochemistry* **1999**, *38*, 5346–5354.
40. Notenboom, V.; Williams, S. J.; Hoos, R.; Withers, S. G.; Rose, D. R. *Biochemistry* **2000**, *39*, 11553–11563.
41. Schramm, V. L. *Curr. Opin. Struct. Biol.* **2005**, *15*, 604–613.